ELASTIC AND VISCOUS PROPERTIES OF RESTING FROG SKELETAL MUSCLE

RICHARD L. MOSS *and* WILLIAM HALPERN, *Department of Physiology and Biophysics, School of Medicine, University of Vermont, Burlington, Vermont 05401*

ABSTRACT The mechanical properties of the resting, whole semitendinosus muscle of the frog have been characterized as functions of both muscle length and temperature. Measurements were made of pseudorandom white noise (PRWN) displacements (<10 Å/half-sarcomere) applied to the muscle and the force responses to these movements. Signal correlation techniques were then used to obtain the dynamic modulus function for the muscle in the frequency range 2.44–320 Hz. This function was represented by a series combination of a Voigt element and a time delay element for tension propagation along the muscle. A dynamic elastic modulus (E), coefficient of damping (B), and tension transmission velocity (V) were measured for resting muscle on the basis of this model.

For each of these parameters, a marked variation with sarcomere length (s) was found. The mean values for E and B at L_0 (s = 2.25 μm) were 1.84 ± 0.24 × 10^5 N/m^2 and 2.33 ± 0.25 × 10^2 Ns/m^2, respectively. Further, B demonstrated a negative temperature dependence, Q_{10} = 0.78 ($P < 0.05$), in the range s = 2.6–3.0 μm, while E was not significantly temperature dependent. The length-dependent variations of E and B are interpreted as deriving from both passive muscle elements and attached crossbridges.

Velocity was calculated at a single displacing frequency for every experiment; the mean value at L_0 and all temperatures was v = 11.7 ± 0.6 m/s. Velocity was also calculated as a function of frequency within several experiments: the results indicate considerable variation of v with frequency.

INTRODUCTION

The sources of tension exerted by stretched, resting skeletal muscle are only partly known. One likely source is the sarcolemma, since sarcolemmal tubes, from which the contractile material has been made to retract, have been shown to exert tension when stretched beyond slack length (Ramsey and Street, 1940; Fields and Faber, 1970). However, tension-length data from this preparation cannot be simply applied to living muscle due to an inability to relate tube length to a corresponding sarcomere length and also because tube sarcolemmal structure is apparently altered from that of sarcolemmae associated with intact muscle fibers. Other studies (Rapoport, 1972;

Dr. Moss' present address is: Department of Muscle Research, Boston Biomedical Research Institute, Boston, Mass. 02114

Podolsky, 1964) on living single frog skeletal muscle fibers have demonstrated sarcolemmal contributions to passive tensions at sarcomere lengths greater than 3.0–3.2 μm. This length is approximately the length at which folds present in the sarcolemma at shorter lengths have been observed to disappear (Dulhunty and Franzini-Armstrong, 1975). Agreement has yet to be reached as to the fraction of total resting tension due solely to the sarcolemma.

Evidence has mounted that suggests the presence of noncontractile, tension-bearing structures within the muscle fiber. Sandow (1966) and Herbst and Piontek (1975) have proposed that the sarcoplasmic reticulum is this kind of structure, based on the dependence of resting tension on the tonicity of the fluid bathing the muscle. Rapoport (1972), using an elastimeter method, characterized an elasticity which he suggested was a property of the myoplasm and which would account for most of the resting fiber elasticity and tension over a broad length range.

Several investigators have reported experimental results that they believe indicate the attachment of crossbridges in both resting skeletal (e.g., Hill, 1968; Haselgrove, 1975) and cardiac (Winegrad, 1974) muscles. Among these is the elastic response first observed by D. K. Hill (1968) in slowly stretched whole sartorius muscle, which he ascribed to a "short-range elastic component" (SREC). Measurements of the stiffness of the SREC at various initial muscle lengths did not, however, give the result expected on the basis of a crossbridge source. Rather than declining as muscle length was increased above the optimum, the stiffness of the SREC remained approximately constant with increasing length. Recently, Moss et al. (1976) have shown that the amplitude of the SREC stiffness in muscle preparations in which the myofibrils have been exposed to the bathing medium increases as the free $[Ca^{2+}]$ is raised, there being no short-range elastic response when $[Ca^{2+}]$ was lowered below 10^{-7} M. These results suggested that the SREC in the intact resting muscle is the property of activated and possibly attached crossbridges.

It is therefore likely that resting muscle stiffness and tension derive from more than a single structural source. The present work was undertaken to characterize the viscoelastic properties of resting muscle as functions of both muscle length and temperature in an attempt to identify the structural sources of the measured properties. The investigative technique used involves pseudorandom signal analysis, as adapted to muscle by Halpern and Alpert (1971), whereby minute length changes are imposed on the muscle by a vibrator driven with a pseudorandom white noise (PRWN) signal. The application of these complex signals to muscle is equivalent to subjecting the muscle to length changes corresponding to a large number of sinusoidal frequencies during the time span of one pseudorandom period. Computer processing of the displacement signal and the corresponding force response, using correlation techniques, results in a complete muscle stiffness transfer function, including both the real and imaginary components, for each discrete frequency contained in the PRWN signal. This information is then analyzed in a way that allows for identification of a viscoelastic mechanical model that behaves analogously to the resting muscle.

METHODS

Preparation

The dorsal heads of semitendinosus muscles were dissected from Vermont *Rana pipiens*, with special care to remove the connective tissue sheath surrounding each muscle. The tendons of the isolated muscle were tied with 6-0 silk to steel connectors (see inset, Fig. 1) for mounting in the experimental chamber. All dissections were performed at room temperature in a chamber filled with phosphate-buffered Ringer of the following ionic composition (millimolar): NaCl, 111.0; KCl, 2.5; $CaCl_2$, 1.8; NaH_2PO_4, 0.45; Na_2HPO_4, 2.5; pH was in the range 7.1–7.3. D-Tubocurarine was dissolved in the bath to a final concentration of 10^{-5} g/ml. The bath solution used during the experiments had the same content.

System Overview

The spatial arrangement of the main components of the experimental system is shown in Fig. 1. The force transducer (*F*) and experimental chamber (*C*) were mounted to a brass block, which in turn was dove-tailed and fixed to an aluminum rail. The displacement transducer (*A*) and vibrator were carried by a similar brass piece free to move longitudinally on another

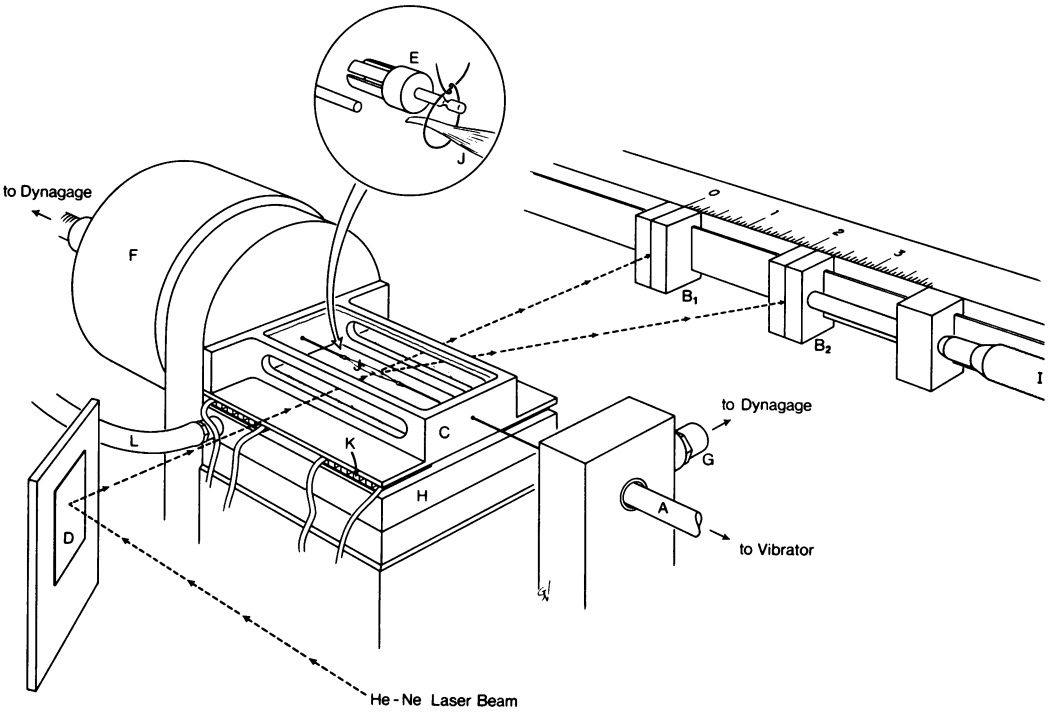

FIGURE 1 Detailed drawing of experimental chamber. *A*, displacement transducer shaft; B_1, block for imaging zero-order beam; B_2, block for imaging first-order line; *C*, experimental chamber; *D*, mirrow; *E*, connector; *F*, force transducer; *G*, displacement transducer coil; *H*, water-cooled heat sink; *I*, micrometer; *J*, muscle; *K*, thermoelectric device; *L*, water outlet. Stimulating electrodes and electrostatic shield for the displacement transducer are not shown. *Inset:* expanded view of muscle connector showing method of muscle attachment.

aluminum rail aligned with the first. Both support pieces were firmly secured to a planed granite block. Precise movements of the displacement assembly relative to the force transducer (as required to change muscle length) were made by means of a micrometer screw arrangement.

Despite the large effective mass of the system and mechanical separation of the rails, transmission paths in parallel with the muscle were found between the vibrator and force transducer. The effects of these spurious pathways were negligible for frequencies up to approximately 420 Hz. Still, the upper limit of the data bandwidth was restricted to 320 Hz to assure the determination of a valid dynamic modulus.

Experimental Chamber

This consisted of a shallow (9.5 mm), rectangular (6.0 × 3.2 cm), hard anodized aluminum well (see Fig. 1). Glass inserts in the walls provided an optical path for laser illumination of the preparation and for imaging the diffracted beam. Holes at the ends of the chamber accepted stainless steel shafts connected to the force transducer and vibrator, the muscle being mounted between these shafts. Close tolerances between the shafts and the chamber walls prevented fluid leakage from the well.

Stimulus

Stimulation of the muscle was achieved by passing current between two platinum strips (1.8 × 53 mm) above and below the muscle. The applied current pulse was approximately rectangular in shape and adjustable in amplitude to a maximum bath current of 2.4 A. Pulse width was set between 0.2 ms at 26.2°C and 0.5 ms at 11.2°C. During tetani the pulses were applied at a 120 Hz rate for 0.4 s at 26.2°C, and 20 Hz for 1.0 s at 11.2°.

Temperature Control

The bath was cooled by four thermoelectric devices (Cambridge Thermionic Corp., Cambridge, Mass., model 801-3959-01), mounted between the outer surface of the floor of the experimental chamber and a water-cooled brass heat sink. Temperature was controlled with a temperature regulator (Yellow Springs Instrument Co., Yellow Springs, Ohio, model 74) and a thermistor located near the chamber floor. Temperatures could be rapidly achieved and were maintained within 0.1°C. The uneven mass distribution about the chamber gave rise to a temperature gradient along the muscle of about 0.15°C, while the vertical temperature gradient across the muscle was less than 0.4°C.

Force Detection

The capacitance force transducer (Hamrell et al., 1975) and detector unit (Dynagage Model DG 600D, Photocon Research Products, Power Sources Division, Whittaker Corp., Denver, Colo.) had a sensitivity of approximately 0.12 V/mN, a compliance of 0.10 μm/mN, a peak-to-peak noise level corresponding to less than 1.8×10^{-5}N, and a predominant natural mechanical frequency of 1.4 kHz. The transducer exhibited a small amount of slow nonsteady drift, making it necessary to adjust the force base line to zero before the recording of data.

Length Detection

The displacement transducer was a capacitor formed by the aluminum shaft of the vibrator and a concentric brass cylinder. This unit was connected to a detector as described in the previous section; the overall system had a sensitivity of 1.97 mV/μm and a noise level equivalent to a peak-to-peak displacement of 0.5 μm.

Absolute sarcomere lengths were measured by a laser diffraction system, as shown in Fig. 1.

The laser (Spectra Physics Inc., Laser Products Div., Mountain View, Calif., model 133; 6,328 Å, 3.5 mW) was mounted on an optical bench parallel to the long axis of the muscle. The laser beam could be made to impinge upon any portion of the muscle by adjusting the position of a flat-plane, front-surface mirror permanently fixed at a 45° angle with respect to the laser beam. Each sarcomere length determination represents the average of five measurements made at points equally spaced along the muscle. Appropriate corrections were made for refraction of the diffracted first-order beam as it passed through materials having different refractive indices, i.e., Ringer solution, glass, and air.

Total muscle length was measured by the method of Kawai and Kuntz (1973). The procedure was to measure the difference in sarcomere lengths (Δs) at two overall muscle lengths, $L_0(s_0 = 2.25\ \mu m)$ and $L_0 + \Delta L$. Then total muscle length at L_0 was calculated with the relationship, $L_0 = (\Delta L/\Delta s)s_0$.

Vibrator and Control Circuits

The vibrator used (Ling Electronics Div., Altec Corp., Anaheim, Calif., specially stiffened model 203) had a stiffness of 90 N/mm and natural resonant frequency of 155 Hz. Displacement feedback and velocity control were used to extend its frequency response and apparent stiffness (Halpern and Alpert, 1971). The amount of each of these was determined by optimizing the response of the system to a step function, and then verifying the fidelity of the displacement signal with respect to the PRWN input wave form. Under these system conditions the effective vibrator stiffness and resonant frequency were approximately 205 N/mm and 1.0 kHz, respectively.

Procedure

Preliminary. Experiments were preceded by a conditioning period of up to 1 h during which the muscle was stimulated with single maximal pulses every 15 s. While this continued, overall muscle length was determined and L_0 set as detailed earlier. After equilibration, stimulus intensity was adjusted to 1.2 times that for maximal twitch tension. Stimulus frequency and pulse duration were then set for fused tetanic responses. Tetanization proceeded at 3-min intervals until succeeding tension traces superimposed. At this point P_0 was defined as the peak developed tension (the average P_0/A[1] for seven muscles at 11.2°C was $1.65 \times 10^5\ N/m^2$).

Experimental. Before the tape recording of data at each muscle length chosen, the muscle was shortened to slack length to obtain a measure of muscle rest tension. Re-extension was followed by a 5–15 min period of re-equilibration to twitches. At longer lengths where stress-relaxation was prominent, resting tension was monitored to ensure that an approximate steady state was reached before recordings were made. PRWN (Hewlett-Packard Co., Palo Alto, Calif., model 3722A noise generator; clock period, 100 μs; sequence length, 409.5 ms) length changes were then applied to the muscle, and the displacement and force signals were simultaneously recorded on separate channels of an FM tape recorder (Honeywell, Inc., Minneapolis, Minn., model 7600).

Once the length study at a given temperature was completed, muscle length was returned to L_0 and maximum tetanic tension was again determined. This permitted assessment of the deterioration of the muscle in terms of percent P_0, a rate of 5%/h and 15% total being the accepted maxima. If this criterion was met, the temperature was altered, the stimulus intensity set, and the muscle allowed to equilibrate for a period of up to 1 h. P_0 was then

[1]Cross-sectional area was calculated from the weight and length of the muscle, assuming a cylindrical shape and a density of $1.0\ g/cm^3$.

found for the new temperature. Individual muscles were studied at as many as three different temperatures. At 26.2° and 16.3°C measurements were made at s = 2.25 μm and 2.4–3.4, in 0.2-μm increments; at 11.2°C, the lengths of 3.6 and 3.8 μm were also included. After each experiment the muscle was cut from its mounts, touched to weighing paper to remove surface water, and then weighed.

Data Processing

Processing of the recorded data for one pseudorandom period involved: (*a*) analog-to-digital conversion on every fourth clock pulse by a minicomputer (Digital Equipment Co., Marlboro, Mass., PDP-8/e), (*b*) transmission of the digitized data to a time-sharing computer (Sigma 6, XDS, Xerox Data Systems, El Segundo, Calif.), (*c*) analysis by a modified version of a program for autocovariance and power spectral analysis (Dixon, 1967), (*d*) plotting of results (Tektronix 4010 graphics terminal, Tektronix Inc., Beaverton, Ore.), and (*e*) permanent copy, as in Fig. 3 (Tektronix 4610 hardcopy unit).

Analysis of the Plotted Results

The complete resting muscle system transfer function over the test range, 2.44–320 Hz, is specified by the stiffness amplitude and phase functions resulting from the pseudorandom data analysis. When plotted against log frequency, the general form of the stiffness amplitude function (Fig. 3*a*) remains constant over the lower frequencies and then increases at higher frequencies. The phase angle (Fig. 3*b*) likewise is constant and near zero at low frequencies, taking on an increasing leading phase in the middle frequency range and finally decreasing at the highest frequencies included. For analysis, the simplest mechanical analogue for this data is a parallel arrangement of a spring and dashpot and a time delay element for mechanical impulse transmission. Then the low frequency behavior of the muscle transfer function would be a property of the elastic element, while the rise in amplitude at higher frequencies represents the increasing contribution of the viscous element. The phase contributed by the time delay element makes the observed phase consistent with that predicted for a simple Voigt element (phase should rise to 90°, force leading; see Halpern and Alpert [1971] for details).

The dynamic stiffness function was multiplied by the ratio of muscle length to cross-sectional area to obtain a dynamic modulus function. Each set of dynamic stiffness data was then fitted by a least mean square error curve, based on the method of Sanathanan and Koerner (1963), to obtain three mechanical parameters. The first was the low-frequency dynamic elastic modulus (E), which for convenience was taken to be the intercept of the fitted amplitude curve with the ordinate at 10 Hz. Next, the coefficient of damping (B), describing the viscous element, was calculated by dividing E by ω_0, where ω_0 is the frequency at which the modulus amplitude is 3 dB above the low frequency modulus (see Halpern and Alpert, 1971). Last, the transmission velocity for force propagation along the muscle was determined. For a Voigt element, the phase at ω_0 is 45°, with force leading displacement. The observed deviation from this value was relegated to the time delay element, where delay in seconds was figured by dividing this phase difference, in radians, by ω_0. Transmission velocity was then calculated as this delay time divided into muscle length.

RESULTS

Length-tension data for the whole semitendinosus muscle is sparse (see, for example, Deleze, 1961). In contrast, length studies of single semitendinosus fibers are numerous, for both active (Ramsey and Street, 1940; Edman, 1966; Gordon et al., 1966)

and passive (Buchthal and Kaiser, 1951) tensions. The latter authors and Fung (1967) indicated that the relationship between passive tension and length could be described by an exponential function; this appears to be the case in the present work.

The mean static resting stress (tension divided by muscle cross-sectional area) data for seven muscles as functions of sarcomere length (s) and strain (L/L_0) at three temperatures are plotted in Fig. 2. Also shown are best fit exponential curves of the form $\sigma = ae^{b\epsilon}$ (σ = resting stress; $\epsilon = s/s_0$; a and b are constants). The mean static resting stress at L_0 for the three temperatures studied is 290 ± 18 N/m^2 (SEM).

An analysis of variance calculated at each sarcomere length indicated no significant difference ($P > 0.05$) between the data at 11.2° and 16.3°C, or between these data combined and that at 26.2°C. Because resting stress is generally believed to be the property of passive muscle elements, a Q_{10} of about 1.03 would be expected. Changes of this magnitude are clearly less than the variability in making the measurements.

Dynamic Elastic Modulus

Dynamic modulus amplitude data for a single experiment is shown in Fig. 3 A, in which is also indicated our estimate of the elastic modulus for this experiment. The corresponding phase function (Fig. 3 B), relating the angle between the system output (force) and input (displacement), shows that the phase is close to zero in the frequency range used to establish the value of the elastic modulus. Finally, Fig. 3C is the coherence function for this experiment and indicates excellent system linearity,

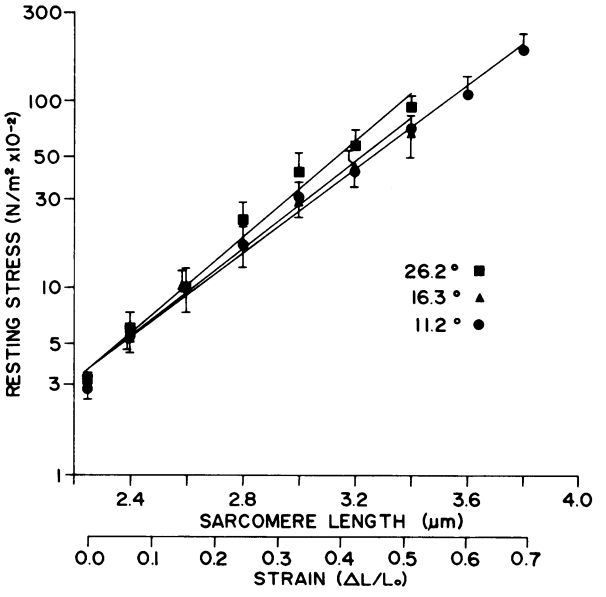

FIGURE 2 Resting stress as a function of sarcomere length and strain ($L - L_0/L_0$) at three temperatures. Straight lines are curves of the form, $\sigma = ae^{b\epsilon}$, fitted to the data. Each point is the mean of five measurements; error bars are + or − SEM.

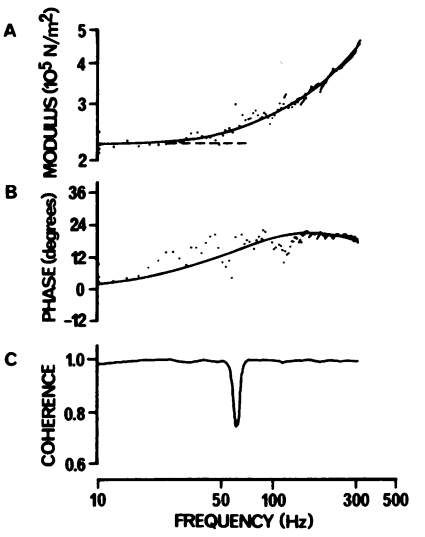

FIGURE 3 Dynamic modulus and coherence functions for single experiment; s = 2.6 μm, temperature = 16.3°C. A. Dynamic modulus amplitude; solid line (here and in B) is the polynomial best fit to the data (see text); dashed line is the low-frequency asymptote used for the elastic modulus measurement. B. Dynamic modulus phase. C. Coherence function. In A–C, data below 10 Hz are plotted on the ordinate for convenience. Also, the data point at 2.44 Hz was not used in the polynomial curve-fitting, as this was usually not coherent.

except for a deviation at 60 Hz due to line noise within the data recording or digitizing systems (Halpern and Alpert, 1971).

The elastic moduli for all muscles are plotted in Fig. 4 A as functions of sarcomere length and strain. At each of the temperatures employed there is an increase in the dynamic elastic modulus as sarcomere length increases from 2.25 to 2.40 μm, followed by nearly constant values in the range s = 2.4–3.0 μm. At all three temperatures, there is a minimum near s = 3.2 μm, above which the modulus increases sharply at greater sarcomere lengths. D. K. Hill (1968) has measured the dynamic elastic modulus of a short-range elastic component (SREC) as a function of length in whole frog sartorius muscle. While not quantitatively comparable because of differences in bathing solution tonicities, this parameter shows qualitatively the same length dependence (see Table 3 of reference) as the elastic modulus of the present study over the range s = 2.4–3.0 μm.

The mean value of all the dynamic elastic modulus measurements at L_0 was 1.84 ± 0.24 × 10^5 N/m^2. This compares reasonably well with: (*a*) D. K. Hill's (1968) value of 2.0 kg/cm^2 (1.96 × 10^5 N/m^2) for the elastic modulus of the SREC at s = 2.4 μm and 6°C; (*b*) Lannergren's (1971) value of 2.28 ± 1.16 × 10^5 N/m^2 for the SREC in a population of single semitendinosus fibers at s = 2.2 μm and 4–7°C; and (*c*) Halpern and Moss' (1976) dynamic elastic modulus of 2.75 × 10^5 N/m^2 for the resting whole sartorius muscle at optimum length and 3°C. An analysis of variance of our data at

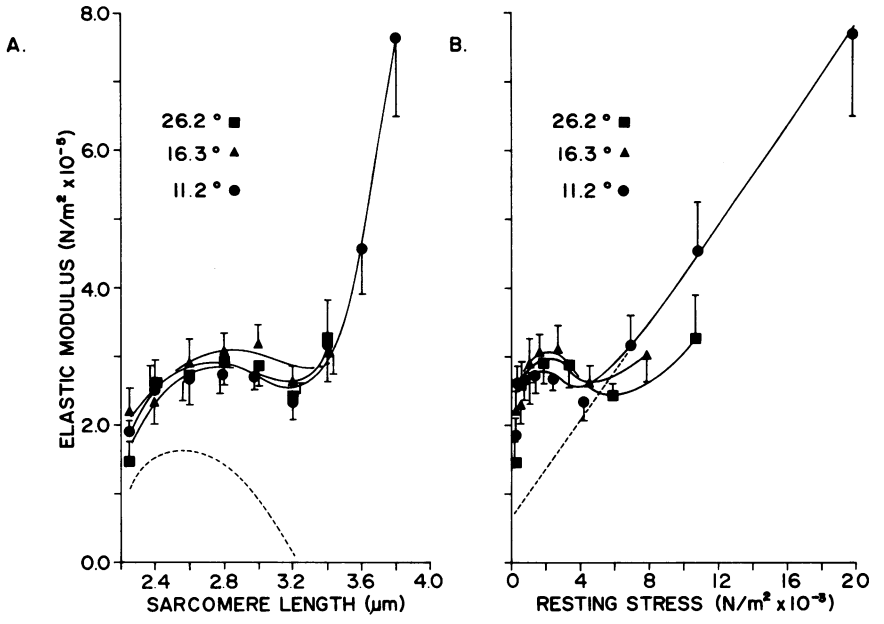

FIGURE 4 A. Dynamic elastic modulus as a function of sarcomere length at three temperatures. B. Dynamic elastic modulus as a function of resting stress. In both A and B, each point is the mean of five experiments; error bars are + or − SEM. Solid lines are polynomial curves fit to these means. The dashed line in Fig. 4 B is the linear extrapolation of the dynamic elastic modulus data at 11.2°C from the high to the low stress range. The extrapolated modulus was subtracted from the mean measured modulus values at 11.2°C to obtain a corrected modulus. These corrected values are plotted versus the sarcomere lengths, which correspond to the measured stress values of B and are represented by the dashed line in Fig. 4 A.

each sarcomere length as a function of temperature showed no significant effect ($P > 0.05$) of temperature on the value of the dynamic elastic modulus.

The dynamic elastic modulus was also plotted against resting stress (Fig. 4 B) in an attempt to uncover possible contributions of exponential elastic elements to the measured values. The basis for this identification would lie in the generally linear dependence of the dynamic elastic modulus on stress for an exponential spring-like element (Fung, 1967; Mirsky and Parmley, 1973). The measurements at 11.2°C were made over a wide stress range and revealed a linear modulus-resting stress characteristic for stresses measured at $s > 3.2\ \mu$m, which indicates an exponential stiffness in this length range. At these sarcomere lengths the amount of thick and thin filament overlap is greatly reduced from the optimum, so that presumably the measured dynamic elastic modulus is mainly the property of either the sarcolemma (Podolsky, 1964) or both the sarcolemma and myoplasm (Rapoport, 1972).

Surely a part of the modulus values measured at $s \leq 3.2\ \mu$m also derives from the elastic element above. However, an approximate correction for this element in the shorter length range is possible if we assume that the linear modulus-stress curve

extrapolates to zero modulus in the stress range that corresponds to $s < 3.2$ μm. We attempted this correction, further assuming that the total measured elasticity represents the sum of the elasticities of parallel structures, thus allowing a simple subtraction of the modulus of the exponential element from the total elastic modulus. When this was done for the data taken at 11.2°C, the result was qualitatively similar to the total modulus-sarcomere length curve for $s < 3.2$ μm, i.e., the elastic modulus rises to a broad peak and then falls as a function of increasing length to $s = 3.2$ μm (corrected curve shown as dashed line in Fig. 4 A).

Coefficient of Damping

The coefficient of damping (B) as a function of sarcomere length (Fig. 5) shows a length dependence similar in form to that of the dynamic elastic modulus. The mean of all data at L_0 is $B = 233 \pm 25$ Ns/m^2. At $s = 2.6$, 2.8, and 3.0 μm, there are significant differences ($P < 0.05$) in B as a function of temperature. Temperature coefficients (Q_{10}'s) calculated for the range 11.2°–26.2°C were 0.76, 0.76, and 0.80, respectively. These values would seem to indicate that active rather than passive muscle elements predominate in determining the value of B. Rosenthal (1964) points out that the coefficients of damping of viscoelastic biological tissues usually decline exponentially as the temperature is raised. In muscle, however, increased temperature

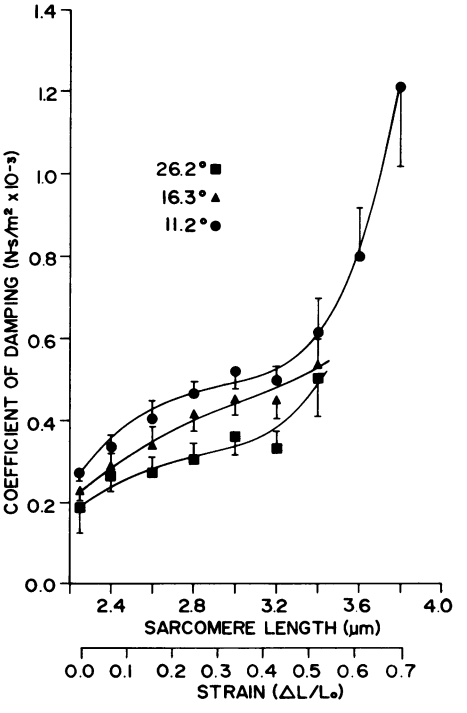

FIGURE 5 Coefficient of damping as a function of sarcomere length. Each point is the mean of five experiments, expressed (+) or (−) SEM. Solid lines are polynomial curves fit to these means.

might also result in altered numbers of attached crossbridges, thereby causing B to change. Since in resting muscle the relative amounts of attached crossbridges and passive structures are not known, the structural source of B cannot be determined solely from the temperature-related data of this study.

The validity of assuming a single damping element for the mechanical model of resting muscle was assessed by calculating B at various displacing frequencies, since B should not vary with the frequency at which it is evaluated. Therefore, several experiments were chosen for calculation of B at the frequencies where, for convenience, the dynamic modulus amplitude was 0.05, 0.10, and 0.15 log units about the low-frequency asymptote. For any given experiment these values were found to agree within about 5%. For example, in the experiment of Fig. 3, B at each of the three amplitudes was 254, 259, and 266 Ns/m^2, respectively.

Transmission Velocity

The average tension transmission velocity at ω_0 calculated for the experiments at L_0 was $V = 11.7 \pm 0.6$ m/s. This value is considerably lower than that obtained by Schoenberg et al. (1974) in semitendinosus fiber bundles (approximately 40 m/s) and whole sartorius muscle (80 m/s). These differences presumably reflect their use of a much higher displacing frequency in making their measurements (see following paragraph for the influence of frequency on v; also, Truong 1974).

Propagation velocities were also calculated within several individual records as a function of the driving frequency. In the low-frequency range in which E was determined, the prediction and observed phases were zero; tension transmission was therefore instantaneous. Above this range, it was found that velocity was finite and remained constant over a frequency band that varied in width from experiment to experiment. In all cases, however, velocity rose at some higher frequency and continued to do so up to 320 Hz. As an example of the latter, the experiment of Fig. 3 yielded velocity values of 15.4 m/s at a total modulus of 2.76×10^5 N/m^2 and 22.6 m/s at 3.10×10^5 N/m^2. The frequencies at which these moduli were measured were 106 and 146 Hz, respectively. The differences in v at various frequencies preclude the possibility that the formula for tension transmission in a homogeneous elastic rod, $v = (E/\rho)$, would pertain in resting muscle.[2]

DISCUSSION

Dynamic Elastic Modulus

Evidence for the presence of calcium activated crossbridges in resting muscle is convincing (Moss et al., 1976; Hill, 1968), though it has yet to be established whether

[2]A further attempt was made to verify that the above equation might apply to either the dynamic elastic modulus for each experiment or the total dynamic modulus amplitude at the frequency ω_0. Thus, $(E)^{1/2}$ was plotted as a function of transmission velocity. For both the dynamic elastic modulus and the total modulus at ω_0, scatter-type plots were obtained, and regression analysis did not establish the predicted linear relationship for either parameter with respect to velocity.

these crossbridges are attached to thin filament sites. In the present study, an interpretation based partly on the presence of attached crossbridges is the best explanation of the variation with length of the resting muscle dynamic elastic modulus. The results cannot be explained on the basis of passive muscle elements alone, for then only a monotonically rising relationship between modulus and increasing length is possible (Fung, 1967), within the strain limits for yielding of these structures. Required to explain the minimum in the dynamic elastic modulus at $s = 3.2\ \mu m$ is a muscle component whose contribution to the measured modulus declines with increasing length. The combined effects of a decreasing number of attached crossbridges and an increasing sarcolemmal stress as sarcomere length is increased can account for this minimum.

Halpern and Moss (1976) and Bressler and Clinch (1974) have shown that in whole sartorius muscle each crossbridge effective in producing a unit of active tension also contributes a unit of elastic modulus to the total measured modulus. These experiments demonstrated that both the isometric, tetanic tension and the dynamic elastic modulus fall off linearly with increasing length above the optimum and that both tension and modulus extrapolated to zero at the same overall muscle length. Thus, evidence for crossbridge attachments in the present study would require that the dynamic elastic modulus, above that of any passive structural contributions, falls off linearly with increasing length, and the concommitant reduction in the amount of thick and thin filament overlap. In Fig. 4 *a*, however, the rising tendency of E at short lengths ($s < 2.6\ \mu m$) is opposite to that predicted for a crossbridge source for the dynamic elastic modulus. The explanation for this most likely lies in the variations of sarcomere structure with length. X-ray diffraction studies of isolated frog semitendinosus fibers by Matsubara and Elliott (1972) show that the lateral spacing of the thick and thin filament lattice decreases inversely with sarcomere length. They also showed that the rate of decrease of separation declines at increasing lengths. Hence, the extra modulus due to active crossbridges could rise, plateau, or even fall in the low length range depending on the relative effects of decreasing separation and decreasing overlap to alter the active crossbridge population. The dynamic elastic modulus in this range (see Fig. 4 A) first rises and would seem to indicate that the effect of decreased separation to increase the number of attached crossbridges dominates at these lengths. As length increases, the reduction in the amount of thick and thin filament overlap could play a larger role, resulting in a falloff in the rate of rise of the dynamic elastic modulus with increasing length. Finally, at the greatest sarcomere lengths where there is still overlap, overlap likely becomes the major tension determinant, causing a decrease in this modulus as length is increased.

That the decrease in filament lattice spacing might in itself lead to increased numbers of attached crossbridges is suggested by the work of Yamada (1970), who demonstrated an increase in resting muscle heat production with the reduction in filamentary lattice volume induced by hypertonic solutions. Further, Clinch (1968) has correlated a portion of the resting tension with the occurrence of increased heat production at long lengths, i.e., the Feng effect (Feng, 1932). These effects as well as our results may arise from an increased probability of interaction of crossbridges with thin filament

sites because of decreased filament spacing, or possibly some other length-dependent event, which for example might lead to an increase in free intracellular calcium (Clinch, 1968).

A difficulty with this interpretation is the apparent contradictory nature of the temperature-related elastic modulus amplitude data, for which no significant temperature dependence was found. In contrast, D. K. Hill (1968) observed a marked increase in the SREC stiffness with increasing temperature. However, Hill's preparations were bathed in hypertonic solutions to enhance the stiffness response, probably by increasing the number of attached crossbridges. Possibly, the high Q_{10} expected of the elastic modulus, if it is the result of an active process, is masked in the present study by the relatively much greater contribution of purely passive viscoelastic muscle structures to this parameter.

Seemingly, most of the dynamic elastic stiffness of the resting semitendinosus muscle, between slack length and $s \cong 3.4\ \mu$m, is due to attached crossbridges. There is no evidence in the present study that resting tension derives from anything but passive muscle structures, and the possibility should be considered that the attached crossbridges in resting muscle bear little or no tension unless they are stretched somehow from their normal, resting positions.

Coefficient of Damping

Viscous effects are well documented in active muscle. For instance the contraction model of Huxley and Simmons (1973) is in large part based on the viscoelastic-type force response of activated living single muscle fibers to a rapid length change. Such effects have seldom been reported for resting muscle. Heinl, et al. (1974) found only an elastic-type force response in length step experiments on relaxed glycerinated ileofibularis fiber bundles from the tortoise. Hill's (1968) investigation of SREC stiffness showed only a small effect of rate of stretch or release on the measured modulus, at least at low stretch velocities. In both of these investigations, however, the mechanical displacements used were probably too slow to uncover the presence of any viscous effects. Apparently, only Buchthal and Kaiser (1951), Halpern and Alpert (1971), and Truong (1974) have previously quantified viscous behavior of resting muscle.

Muscle viscosity may derive from passive muscle structures or a combination of passive elements and attached crossbridges. In either event, for data taken at sarcomere lengths of about 3.4 μm and above, the source is assumed to be mainly passive (see Fig. 5), since the amount of thick and thin filament overlap is small in this region. To determine the nature of the viscosity in the length range of overlap, it is helpful to consider the possible sources of viscosity in muscle. First, the myoplasm, as a fluid, has a measurable viscosity, reported by Giese (1963) to be 29 cP and 5×10^5 cP by Buchthal and Kaiser (1951).

Another likely source of viscosity is the action of adjacent thick and thin filaments to produce a shearing force in the intervening fluid as they slide past one another. For example, as a simplistic model consider two parallel plates where $F = \eta a v/x$. F is the shearing force generated; η the viscosity of the fluid between

the plates; a the area over which F acts; v the velocity at which the plates are moving; and x the distance between the plates. The coefficient of damping (B) may be substituted into this relationship since $Bv = F$. Then, $Bv = vav/x$. Thus, B is directly proportional to a and inversely related to x. Of course, the thick and thin filaments are not parallel plates, and it is difficult to place values on a and x. However, if it is assumed that x is proportional to the filamentary lattice spacing, d, and that a is proportional to the amount of thick and thin filament overlap, some qualitative statements may then be made concerning the relative magnitude of this type of viscosity with increasing muscle length. From the above, B is inversely proportional to d. Matsubara and Elliott (1972) showed that sarcomere length is proportional to $1/d^2$, so that B would then be proportional to $s^{1/2}$. Knowing B at any sarcomere length now permits prediction of B at any other sarcomere length by a simple proportion. For example, B at 11.2°C and 2.25 μm is 0.27 Ns/m^2. Therefore, at 3.0 μm, B should be 0.31 Ns/m^2. The decreased amount of overlap at 3.0 μm (ignoring the presumably secondary effect due to decreased separation between adjacent thick filaments or adjacent thin filaments) will further decrease the value expected for B because of the decreased area of interaction. Thus, by simple proportion, B at $s = 3.0\ \mu$m is 0.23 N-s/m^2; however, the measured B is 0.52 N-s/m^2. Given the assumptions necessary to make the calculations, it appears that this source does not account for the substantial rise in viscosity found as the amount of thick and thin filament overlap is reduced (Fig. 5).

A third possibility to be considered here is the viscous contribution of parallel arrays of structural filaments, of which collagen in the sarcolemma is the main element (Mauro and Adams, 1961). Pure collagen is viscoelastic in nature (Gow, 1972), and it is likely a primary contributor to the coefficient of damping measured at $s \geq 3.2\ \mu$m, the length at which the sarcolemma begins to contribute significantly to the resting stress (Podolsky, 1964; Rapoport, 1972).

Viscous forces primarily of passive origin do not account for the results of this study. Some portion of the resting muscle viscosity may derive from attached crossbridges. Each attached crossbridge would contribute an amount of viscosity, the sum of attached bridges yielding the total viscosity, or coefficient of damping. The data of Halpern and Alpert (1971), in which B was found to be proportional to active stress, and presumably to the number of attached crossbridges, support this hypothesis. They also present data demonstrating a strong correlation in activated muscle between the magnitudes of B and the dynamic elastic modulus, which is known to be proportional to active tension (Halpern and Moss, 1976; Bressler and Clinch, 1974).

The exact nature of a crossbridge-derived viscosity, if one exists in resting muscle, is difficult to resolve, whether it would be an apparent viscosity as envisioned by Huxley and Simmons (1973) or a result of the crossbridges moving or being moved through myoplasm. The latter cannot be quantified because there is a decided lack of *in situ* crossbridge geometrical information. Also, if this is a source of viscosity, the amount contributed may or may not vary with muscle length depending on whether the viscosity was primarily derived from attached or unattached crossbridges.

Tension Transmission Velocity

Displacing frequency has no effect on the transmission velocity, which is measured in a purely elastic material when there are no wave reflections. However, velocity will be frequency dependent in a viscoelastic body. Our work indicates a substantial influence of frequency on velocity in resting muscle. Further, there is neither a unique velocity nor a simple relationship between the dynamic modulus and velocity in any single muscle.

A general problem regarding tension transmission velocities is that the structures that carry the tension waves have yet to be defined. For the active muscle, the suggestion is clear that crossbridges are primarily responsible for tension propagation. Halpern and Alpert (1971) and Schoenberg et al. (1974) found velocity values five to six times (at 0°C) and four times greater (at 6°C), in tetanically activated than in resting muscle. It seems likely as well that attached crossbridges are in some degree responsible for the velocity of transmission in resting muscle. However, the contributions of bridges relative to other possible tension-bearing structures such as sarcolemma, sarcoplasmic reticulum, or even structured muscle water are not known. One can envision that either the tension-transmitting properties of crossbridges and passive elements add in parallel, as the stiffness of these structures is usually assumed to do, or that velocity is determined by the stiffest element in the muscle.

This research was supported by National Institutes of Health grants AM#17163 and HE-10892-04.

Received for publication 23 June 1976 and in revised form 9 November 1976.

REFERENCES

BRESSLER, B. H., and N. F. CLINCH. 1974. The compliance of contracting skeletal muscle. *J. Physiol. (Lond.).* **237**:477–493.

BUCHTHAL, F., and E. KAISER. 1951. The rheology of the cross striated muscle fibre with particular reference to isotonic conditions. *Dan. Med. Bull.* **21**(7):1–318.

CLINCH, N. F. 1968. On the increase in rate of heat production caused by stretch in frog's skeletal muscle. *J. Physiol. (Lond.).* **196**:397–414.

DIXON, N. J. 1967. BMD02T autocovariance and powerspectral analysis. *In BMD Biomedical Computer Programs.* University of California Press, Berkeley, Calif. 459–482.

DELEZE, J. B. 1961. The mechanical properties of the semitendinosus muscle at lengths greater than its length in the body. *J. Physiol. (Lond.).* **158**:154–164.

DULHUNTY, A. F., and C. FRANZINI-ARMSTRONG. 1975. The relative contributions of the folds and caveolae to the surface membrane of frog skeletal muscle fibers at different sarcomere lengths. *J. Physiol. (Lond.).* **250**:513–539.

EDMAN, K. A. P. 1966. The relation between sarcomere length and active tension in isolated semitendinosus fibres of the frog. *J. Physiol. (Lond.).* **183**:407–417.

FENG, T. P. 1932. The effect of length on the resting metabolism of muscle. *J. Physiol. (Lond.).* **74**:441–454.

FIELDS, R. W., and J. J. Faber. 1970. Biophysical analysis of the mechanical properties of the sarcolemma. *Can. J. Physiol. Pharmacol.* **48**:394–404.

FUNG, Y. C. B. 1967. Elasticity of soft tissues in simple elongation. *Am. J. Physiol.* **213**:1532–1544.

GIESE, A. C. 1963. Cell Physiology. W. B. Saunders Company, Philadelphia, Pa. 199–202, 204.

GORDON, A. M., A. F. HUXLEY, and F. J. JULIAN. 1966. The variation in isometric tension with sarcomere length in vertebrate striated muscle. *J. Physiol. (Lond.).* **184**:170–192.

GOW, B. S. 1972. The Influence of Vascular Smooth Muscle on the Viscoelastic Properties of Blood Vessels. *In Cardiovascular Fluid Dynamics, Vol. 2.* D. H. Bergel, editor. Academic Press, Inc., New York and London.

HALPERN, W., and N. R. ALPERT. 1971. A stochastic signal method for measuring dynamic mechanical properties of muscle. *J. Appl. Physiol.* **31**:913–925.

HALPERN, W., and R. L. MOSS. 1976. Elastic modulus and stress relationships in stretched and shortened frog sartorii. *Am. J. Physiol.* **230**:205–210.

HAMRELL, B. B., R. PANAANAN, J. TRONO, and N. R. ALPERT. 1975. A stable, sensitive, low-compliance force transducer. *J. Appl. Physiol.* **38**:190–193.

HASELGROVE, J. C. 1975. X-ray evidence for conformational changes in the myosin filaments of vertebrate striated muscle. *J. Mol. Biol.* **92**:113–143.

HEINL, P., H. J. KUHN, and J. C. RUEGG. 1974. Tension responses to quick length changes of glycerinated skeletal muscle fibers from the frog and the tortoise. *J. Physiol. (Lond.).* **237**:243–258.

HERBST, M., and P. PIONTEK. 1975. Studies on the origin of latency relaxation and resting tension of skeletal muscle: the effect of hypotonic solutions. *Life Sci.* **16**:891–902.

HILL, D. K. 1968. Tension due to interaction between the sliding filaments in resting striated muscle. The effect of stimulation. *J. Physiol. (Lond.).* **199**:637–684.

HUXLEY, A. F., and R. M. SIMMONS. 1973. Mechanical transients of muscular force. *Cold Spring Harbor Symp. Quant. Biol.* **37**:669–680.

KAWAI, M., and I. D. KUNTZ. 1973. Optical diffraction studies of muscle fibers. *Biophys. J.* **13**:857–876.

LANNERGREN, J. 1971. Low-level activation and mechanical properties of muscle. *J. Gen. Physiol.* **58**: 145–162.

MATSUBARA, I., and G. F. ELLIOTT. 1972. X-ray diffraction studies on skinned single fibers of frog skeletal muscle. *J. Mol. Biol.* **72**:657–669.

MAURO, A., and W. R. ADAMS. 1961. The structure of the sarcolemma of the frog skeletal muscle fiber. *J. Biophys. Biochem. Cytol.* **10**:177–186.

MIRSKY, I., and W. M. PARMLEY. 1973. Assessment of passive elastic stiffness for isolated heart muscle and the intact heart. *Circ. Res.* **33**:233–243.

MOSS, R. L., M. R. SOLLINS, and F. J. JULIAN. 1976. Calcium activation produces a characteristic response to stretch in both skeletal and cardiac muscle. *Nature (Lond.).* **260**:619–620.

PODOLSKY, R. J. 1964. The maximum sarcomere length for contraction of isolated myofibrils. *J. Physiol. (Lond.).* **170**:110–123.

RAMSEY, R. W., and S. F. STREET. 1940. The isometric length-tension diagram of isolated skeletal muscle fibers of the frog. *J. Cell. Comp. Physiol.* **15**:11–34.

RAPOPORT, S. I. 1972. Mechanical properties of the sarcolemma and myoplasm in frog muscle as a function of sarcomere length. *J. Gen. Physiol.* **59**:559–585.

ROSENTHAL, D. 1964. Introduction to Properties of Materials. D. van Nostrand Company, New York. 196.

SANATHANAN, C. K., and J. KOERNER. 1963. Transfer function synthesis as a ratio of two complex polynomials. *IEEE Trans. Auto Control.* **8**:56–58.

SANDOW, A. 1966. Latency relaxation: A brief analytical review. *Med. Coll. Va. Q.* **2**:82–89.

SCHOENBERG, M., J. B. WELLS, and R. J. PODOLSKY. 1974. Muscle compliance and the longitudinal transmission of mechanical impulses. *J. Gen. Physiol.* **64**:623–642.

TRUONG, X. T. 1974. Viscoelastic wave propagation and rheologic properties of skeletal muscle. *Am. J. Physiol.* **266**:256–264.

WINEGRAD, S. 1974. Resting sarcomere length-tension relation in living frog heart. *J. Gen. Physiol.* **64**: 343–355.

YAMADA, K. 1970. The increase in the rate of heat production of frog's skeletal muscle caused by hypertonic solutions. *J. Physiol. (Lond.).* **208**:49–64.